16th World Conference on Earthquake, 16WCEE 2017
Santiago Chile, January 9th to 13th 2017
Paper N° 2135
Registration Code: S-X1463159499

AFTERSHOCK COLLAPSE PERFORMANCE OF INFILL FRAMES

H. Burton [1], M. Sharma [2] and S. Sreekumar [3]

[1] Assistant Professor, Department of Civil and Environmental Engineering, University of California, Los Angeles, hvburton@ucla.edu
[2] Structural Engineer, Optimum Design Private Limited, Noida, India, mayanksharma@g.ucla.edu
[3] Design Engineer, Englekirk Structural Engineers, Los Angeles, CA, ssnarayan379@ucla.edu

Abstract

The aftershock collapse safety of a building can inform the decisions of owners and users regarding reoccupancy after an earthquake, thereby affecting the recovery process. This paper seeks to quantify the aftershock collapse performance of two reinforced concrete frame buildings with infills. After assessing their collapse safety in the intact state, the residual collapse capacity following mainshock damage is evaluated by conducting incremental dynamic analysis to collapse using mainshock-aftershock ground motion sequences. The studied buildings are representative of modern design and construction of residential buildings in Noida, India and vary based on the configuration of infill panels (full height and soft-story configurations). The rate of decline in collapse capacity is measured based on the median spectral acceleration at collapse for the main shock damaged building normalized by that of the intact case as a function of the mainshock intensity. The increase in the conditional probability of collapse is also used as a metric for quantifying the decline in collapse safety. The study finds that the presence of a soft and weak first story significantly increases the aftershock collapse vulnerability. Among the engineering demand parameters recorded during the mainshock analyses, the peak column hinge rotation was found to have the highest correlation with the reduction in collapse performance for the damaged soft story building. For the building with full height infill, all mainshock response parameters were found to have comparable correlation with the aftershock collapse vulnerability.

Keywords: aftershock collapse performance, seismic resilience, reinforced concrete, infill frames, ground motion sequences

1. Introduction

Recent earthquake sequences such as the ones that occurred in Christchurch (2010-2011), Tohoku (2011) and Gorkha (2015), have highlighted the importance of considering both mainshock and aftershock ground motion hazard in the seismic design and performance assessment of buildings. Aftershock events have been shown to exacerbate the damage caused by mainshocks and in some cases have led to collapse. The vulnerability to aftershock collapse also influences the post-mainshock decisions of owners and users regarding reoccupancy of a building after an earthquake.

Various aspects of aftershock earthquake effects have been investigated in previous studies including (1) ground motion selection [1,2], (2) hazard and risk characterization [3,4] (3) approaches to quantifying the residual capacity of mainshock-damaged buildings [5-7] and (4) aftershock performance assessment for specific construction types including reinforced concrete [8,9], steel [7,9,11] and woodframe [12] buildings. Tesfamariam et al. [2] conducted a parametric study on the seismic response of reinforced concrete frame buildings with infills subjected to mainshock-aftershock sequences. The objective of this study was to assess the change in fundamental period and interstory drift demands between the mainshock and aftershock. The present study aims to quantify the aftershock collapse safety of a two 6-sotry reinforced concrete frame buildings with infills. The first is constructed with full height infill panels and the second with partial height infill, creating the presence of a soft and weak story.

2. Description and Structural Modeling of Building Cases

The aftershock collapse performance of two 6-story infill frame buildings is investigated as part of this study. The buildings were designed in accordance with the Indian Standard for Earthquake Resistant Design of

Structures [13] as part of a larger study on the seismic performance assessment of infill frame buildings in Noida, India [14]. Noida is located in a region of moderate seismicity and has a long history of earthquakes originating both locally and as far as the Himalayas [15]. A seismic zone factor Z = 0.24 is used based on the location of Noida in a region of Zone 4 seismicity and a response reduction factor R = 5 is used in accordance with Table 7 of IS 1893-2000. An importance factor I = 1.0 was assumed.

The architectural layout and structural plan for the studied buildings are shown in Fig. 1. The typical story height is 3.7 m and all bays are 3.7 m wide. Two variants of this building are investigated: one with full height infill panels and another with the infill panels terminating at the second story creating the presence of a soft and weak first story. All infill panels are 220 mm thick with a prism compressive strength of 3.5 MPa. The compressive strength for concrete is taken to be 20.7 MPa and the yield strength of the steel reinforcement is 413.7 MPa. All beams have cross sectional dimensions of 355 mm x 455 mm, with 3-#4 longitudinal bars top and bottom and #3 stirrups spaced at 405 mm. The columns in the bottom three stories have cross sectional dimensions of 405 mm x 405 mm with 8-#6 longitudinal bars. In the top three stories, the columns are 355 mm x 355 mm with 8-#5 longitudinal bars. All columns have #3 ties spaced at 305 mm apart. With the exception of the presence of infill panels in the first story, the design details of the two variations of the 6- story buildings are identical. The design cases were developed based on the results of a field survey of residential buildings in Noida and reviewed by local practicing engineers.

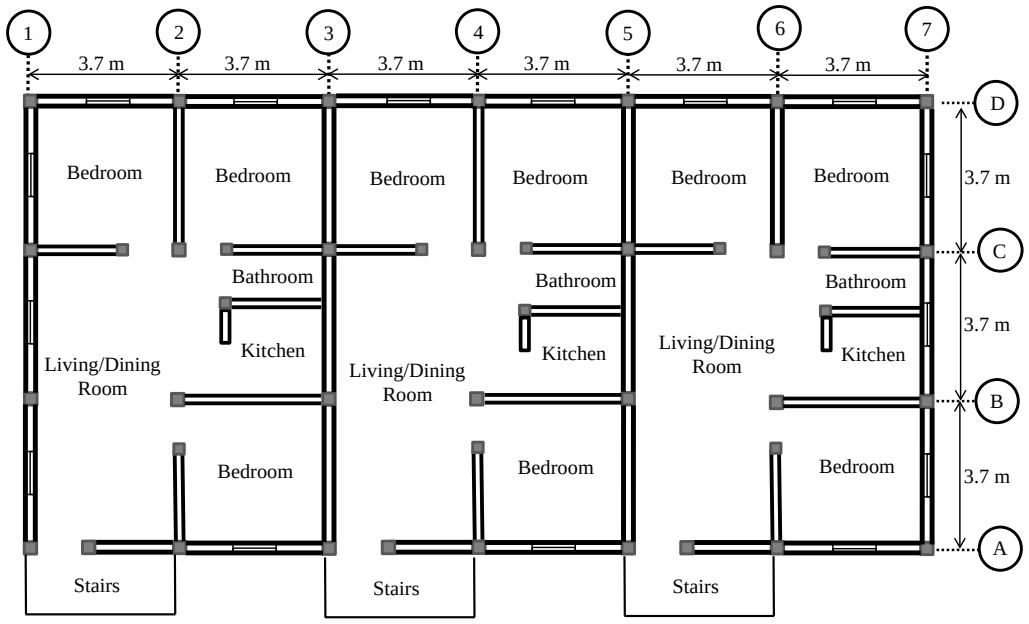

(a)

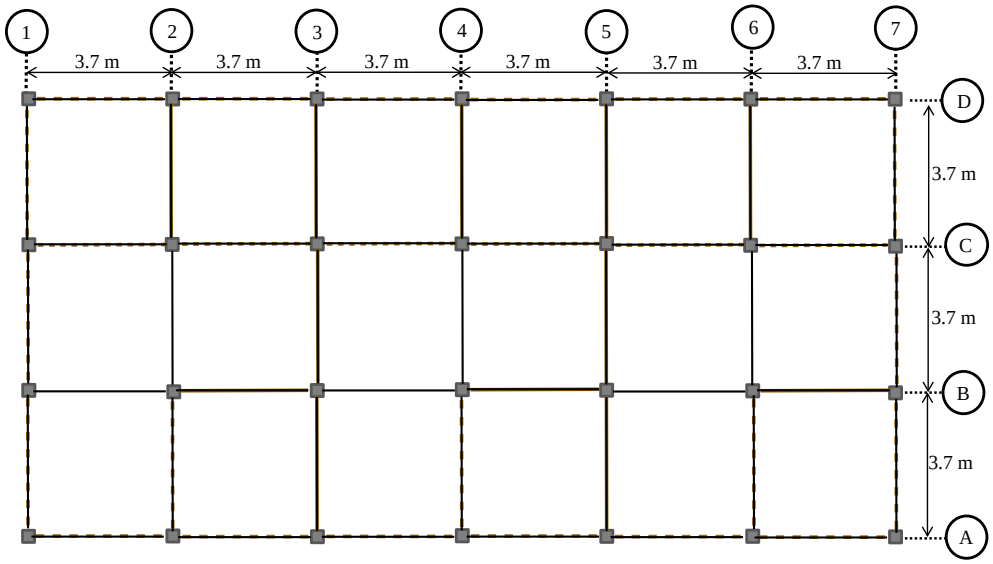

(b)

Fig. 1 – 6-story multi-family residential building (a) architectural layout and (b) structural floor plan

Structural models of the exterior longitudinal frame Line A developed in *OpenSees* are used to simulate the nonlinear dynamic response of the building. A leaning column is used to incorporate P-Δ effects. The elevation for the 6-story frame with full height infill panels is shown in Fig. 2. Beams and columns are idealized using elastic elements with concentrated flexural plastic hinges with the Ibarra-Krawinkler [16] hysteretic model to capture nonlinear moment-rotation behavior. The parameters for the reinforced concrete beams and columns are obtained using the predictive equations developed by Haselton et al. [17] through calibration to experimental data. The infill panels are modeled using a pair of inelastic compression-only struts in each direction that incorporate strength and stiffness deterioration. The dual compression struts (see Fig. 2) capture the column-infill interaction that can cause shear failure of the columns. The Ibarra-Krawinkler hysteretic model is adapted and used to capture the nonlinear behavior of the infill compression struts. The analytical relationships developed by Saneinejad and Hobbs [18] are used to compute the capping strength, and the initial stiffness, of the infill struts. The guidelines by Burton and Deierlein [19] are used to obtain the other strut model parameters including the ratio of capping strength to yield strength, the ratio of capping displacement to yield displacement, and the ratio of post-capping stiffness to yield stiffness. The strut model parameters were established based on calibration to data from 14 experimental tests on infill frames.

A zero-length shear spring is placed in series with the flexural hinges at the ends of the columns and assigned a rigid-softening shear force versus deformation model [19]. Shear failure is followed by a negative post-peak slope that captures the shear strength degradation. A high initial stiffness is used for the elastic region, i.e., zero deformation is assumed in the spring up to the shear strength of the column. This assumption is consistent with the fact that column shear failure in infill frames typically occurs at very low drift levels. The deformation parameters for the shear spring are derived from the modeling criteria provided in Tables 6–8 of ASCE/SEI 41 (2007). Elwood et al. [21] developed a supplement to ASCE/SEI 41 related to existing RC buildings that is based on experimental evidence and empirical models. The supplement includes modeling criteria for columns that have experienced shear failure before flexural yielding. The axial failure of columns that follows the complete degradation of shear strength is not incorporated in the structural model.

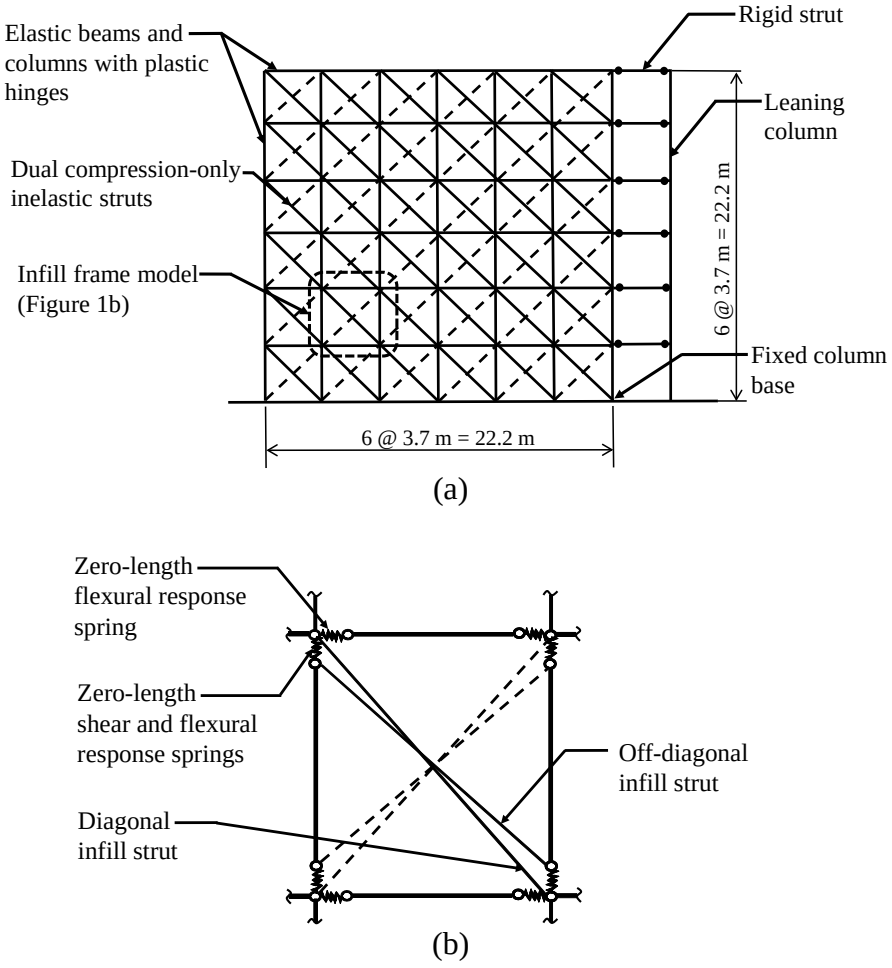

Fig. 2 – (a) Schematic overview of OpenSees model for 6-story building with full height infill panels including (b) the interface between the infill strut and frame elements

3. Collapse Performance Assessment of Undamaged Buildings

To establish a baseline assessment of collapse performance, incremental dynamic analysis (IDA) was carried out on the intact building variants and the statistical distribution of the collapse intensity was obtained. Nonlinear response analyses were conducted using the set of 22 far-field ground motion pairs (44 ground motions applied to 2D models) and the scaling method of FEMA P695 [22]. The spectral acceleration level corresponding to the 1st mode period of the building is used as the ground motion intensity measure. Two definitions of collapse are considered in this study. The first is the sidesway collapse mode for which dynamic instability occurs during nonlinear response history analysis and the lateral displacement of the structure increases without bounds. The second is the "first component failure" mode where the building is considered to be in the collapse limit state when a single structural component succumbs to a particular failure mechanism. For this study, in addition to the case of dynamic instability, collapse was assumed to occur when the column shear strength has reduced to zero.

Fig. 3 shows the collapse fragility curve for the 6-story buildings in their intact or undamaged state. The total system collapse uncertainty was taken as the square root sum of squares of the modelling uncertainty and the record to record dispersion. A spectral shape factor was applied in accordance with Table 7-1a of FEMA P695. After accounting for modelling uncertainty and spectral shape, the probability of collapse at the spectral acceleration corresponding to the MCE hazard level is 5.8% and 52.8% for the full- and partial height infill buildings respectively. The presence of a soft story significantly reduces the collapse safety with the conditional

probability of collapse at the MCE increased by a factor of about 10. Of the 44 ground motions used to analyse the buildings, only one collapsed as a result of column shear failure in the full height infill panel model and there were no cases where collapse was induced by column shear failure in the soft-story model.

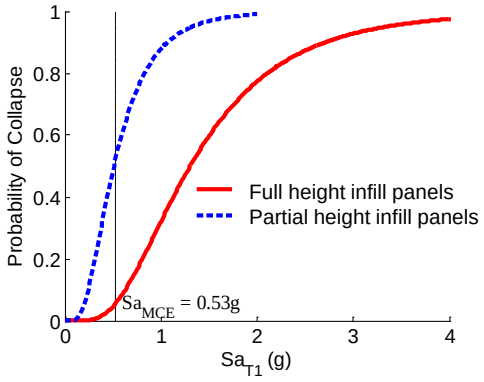

Fig. 3 – Collapse fragility curves for the undamaged 6-story buildings including the effect of modeling uncertainty and spectral shape factor

4. Aftershock Collapse Performance

The aftershock collapse vulnerability that results from changes in the strength, stiffness and overall behavior of mainshock-damaged buildings is also evaluated. *IDA* to collapse is performed using sequential inertial loading where, at each intensity, the structural model is subjected a "mainshock" followed by an "aftershock" ground motion. The collapse fragility curve for a structure subjected to a single realization of damage is obtained using a single mainshock ground motion scaled to a single intensity $\left(Sa_{T1,MS}\right)$ and multiple aftershock ground motions with incrementally increasing intensity $\left(Sa_{T1,AS}\right)$. Multiple realizations of mainshock damage are used to evaluate the effect of various types and levels of damage on the reduction in collapse capacity. The extent and distribution of damage is varied by using multiple mainshock ground motions scaled to different intensities. Artificial MS-AS sequences are generated using the set of FEMA P695 far field ground motions as both the mainshock and aftershock motions. A total of 9680 sequences was generated for each building by combining each of the 44 mainshock ground motions scaled to 5 different intensity levels with the same set of 44 aftershock ground motions. The mainshock intensity for a given ground motion is defined relative to the collapse capacity of the intact structure for that particular ground motion. This is done to ensure that collapse does not occur during the mainshock. The mainshock intensities for the building with full height infill panels are taken to be 20%, 50%, 80%, 90% and 95% of the collapse capacity of the respective intact building, when subjected to the individual mainshock ground motion alone. As will be discussed later in the paper, the soft story building is much more susceptible to significant reductions in its collapse safety due to mainshock damage. As such, the mainshock intensities for the soft-story building are taken to be 20%, 50%, 65%, 75% and 85% of their collapse capacity in the intact state.

The decline in collapse safety of a building after being subjected to a mainshock earthquake is directly related to the level and distribution of damage that occurs. Displacement-based engineering demand parameters (EDPs) are known to be effective predictors of structural damage. Story drift (transient and residual) ratios and component deformation demands are used to assess global and local structural damage. Fig. 4 shows the median profile of peak story drift ratios (SDR) for the two buildings, recorded during the mainshock analyses. For the full height infill panel building, there is a gradual increase in *SDR* moving from upper to lower stories, although the change is more pronounced at higher intensities. In contrast, drift demands are almost exclusively concentrated in the first story at all intensities for the partial-height infill panels building, highlighting the effect of a soft and weak first story on the distribution of mainshock damage.

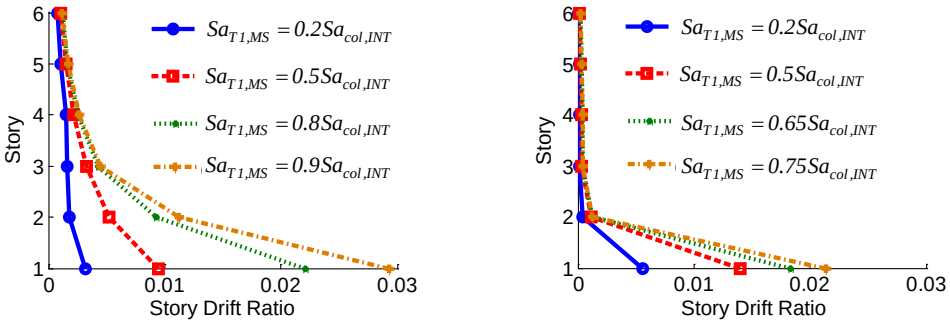

(a) (b)

Fig. 4 – Median peak story drift profiles from mainshock response history analyses for 6-story buildings with (a) full and (b) partial height infill

The presence of a soft and weak story also affects the distribution of local structural damage. Fig. 5 shows the median of the peak deformation demand (normalized by the capping strength) for various structural components in the two 6-story buildings, recorded during the mainshock analyses. It shows that, for the full-height infill panel building, the axial deformation in the infill struts are as high as 4.5 times the capping deformation, which suggests that there is significant strength degradation in the infill panels. For the same building, the rotation demands in the beam hinges are generally higher than the columns, suggesting a more distributed yielding mechanism. The opposite is true for the soft story building, where the highest deformation demands are in the column hinges, which is consistent with the formation of a story mechanism. Additionally, there is also very little deformation demands in the infill panels (located above the 1st story).

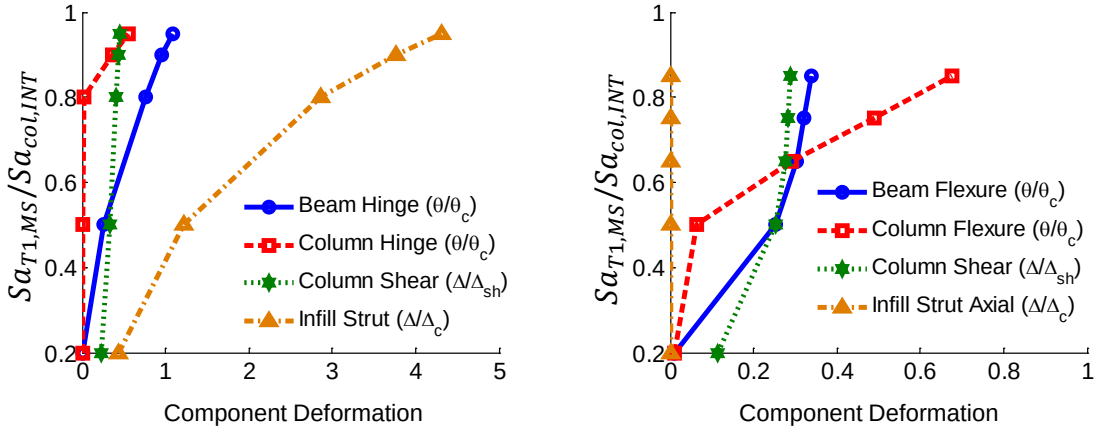

(a) (b)

Fig. 5 – Median peak component deformations from mainshock response history analyses for 6-story buildings with (a) full and (b) partial height infill

Two metrics are used to quantify the reduction in collapse safety of the mainshock-damaged buildings. The residual collapse capacity index (κ) is taken as the ratio between the median collapse capacity of the mainshock-damaged building $\left(\hat{S}a_{col,DMG}\right)$ to that of the intact case $\left(\hat{S}a_{col,INT}\right)$.

$$\kappa = \frac{\hat{S}a_{col,DMG}}{\hat{S}a_{col,INT}} \quad (1)$$

The ratio of the probability of collapse at the *MCE* of the mainshock-damaged building $\left(P_{col,DMG}\right)$ to that of the intact case $\left(P_{col,INT}\right)$ is also used to assess the reduction in collapse safety.

$$\gamma = \frac{P_{col,DMG}}{P_{col,INT}} \tag{2}$$

Fig. 6a shows examples of collapse fragility curves for the intact and mainshock-damaged cases for the soft-story building, corresponding to a single mainshock ground motion scaled to four different intensities. It shows that, as the intensity of the mainshock ground motion increases, the collapse performance of the building worsens as a result of the escalation in mainshock damage. For the case where the mainshock is scaled to 50% of the collapse capacity, the probability of collapse at the *MCE* only increases by 4% $(\gamma = 1.04)$. At mainshock intensities corresponding to 65% and 75% of the collapse capacity, the degradation in collapse safety is more significant with the *MCE* level probability of collapse increasing by 20% $(\gamma = 1.2)$ and 40% $(\gamma = 1.4)$ respectively. The median spectral acceleration at collapse is reduced by 2% $(\kappa = 0.98)$, 11% $(\kappa = 0.89)$ and 26% $(\kappa = 0.74)$ when the mainshock intensity is 50%, 65% and 75% of the intact collapse capacity respectively.

Fig. 6b compares the reduction in collapse safety due to mainshock-damage for the two building cases. It shows a plot of the median spectral acceleration at collapse for each mainshock-damaged building $\left(\hat{S}a_{col,DMG}\right)$, normalized by that of the intact case, versus the mainshock ground motion intensity normalized by the *MCE* hazard level. At each mainshock intensity, the median collapse capacity is computed based on 1936 sequences (44 mainshocks and 44 aftershocks). The effect of the mainshock intensity is assessed based on the slope of each of the lines shown in the plot, which can be interpreted as the incremental reduction in collapse safety (as measured by κ) per unit increase in the mainshock spectral acceleration (normalized by the *MCE*). For the building with full height infill panels, the reduction in collapse safety is almost negligible at the lowest mainshock intensity. Even for the soft and weak story building case, the median collapse capacity of the damaged condition is within 10% of the intact state for the lowest mainshock intensity. The increase in mainshock intensity affects the residual collapse capacity of the soft story building more than its full height infill counterparts. For example, the effect of mainshock intensity on the aftershock collapse vulnerability (as measured by the averaged slope of the line connecting the data points in Fig. 6b for a given building) is approximately four times greater when there is a soft and weak 1st story.

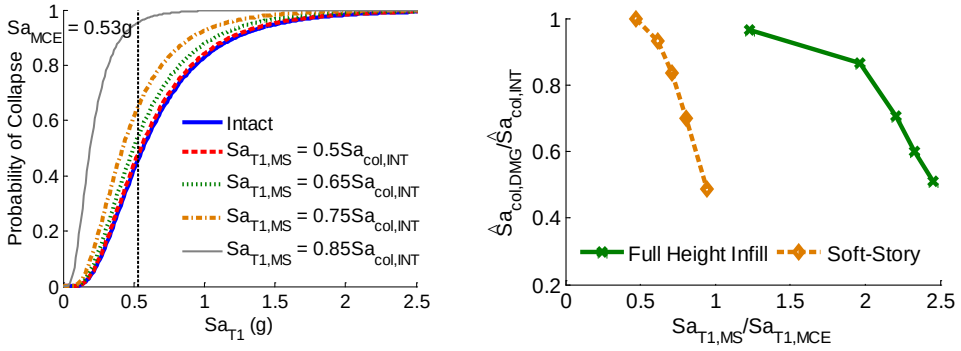

(a) (b)

Fig. 6 – (a) Collapse fragility curves for intact and mainshock-damaged soft-story building and (b) plots showing the median collapse capacity of both mainshock-damaged buildings normalized by that of the intact case as a function of the mainshock intensity

The response demands recorded during the mainshock analyses can serve as indicators of the reduction in the collapse safety of the damaged buildings. Figs. 7 through 11 show the individual relationship between the

mainshock structural response parameters and the reduced collapse safety for the two buildings including the correlation coefficients. Each data point corresponds to a single mainshock ground motion scaled to a particular intensity followed by an *IDA* of aftershock ground motions. There are a total of 220 mainshocks corresponding to 44 ground motions scaled to five different intensity levels. Fig. 7 shows that the aftershock collapse safety of the soft-story building has a much stronger relationship with the peak transient drift, where the correlation coefficient is 0.81 compared to 0.58 for the full-height infill building. Moreover, a clear trend emerges at a peak story drift ratio of 1% for the soft-story building compared to approximately 2% for its full-height infill counterpart. A similar comparison can be made between the two buildings for the residual story drift ratio and the infill strut peak axial deformation, both of which are almost perfectly correlated with the peak transient story drift. As noted earlier and observed in Fig. 9, the beam hinge plastic rotation demands from the mainshock analysis are significantly higher for the full-height infill building. This observation is consistent with the fact that the soft-story building is more susceptible to a single story mechanism that results from hinging in the columns. Fig. 9 shows that the correlation between γ and the maximum beam plastic hinge rotation is only slightly higher for the soft-story building. The mainshock peak column hinge rotation has the highest correlation with the aftershock collapse vulnerability among all component-level response parameters for both building types. However, the correlation is almost 70% greater for the soft-story building.

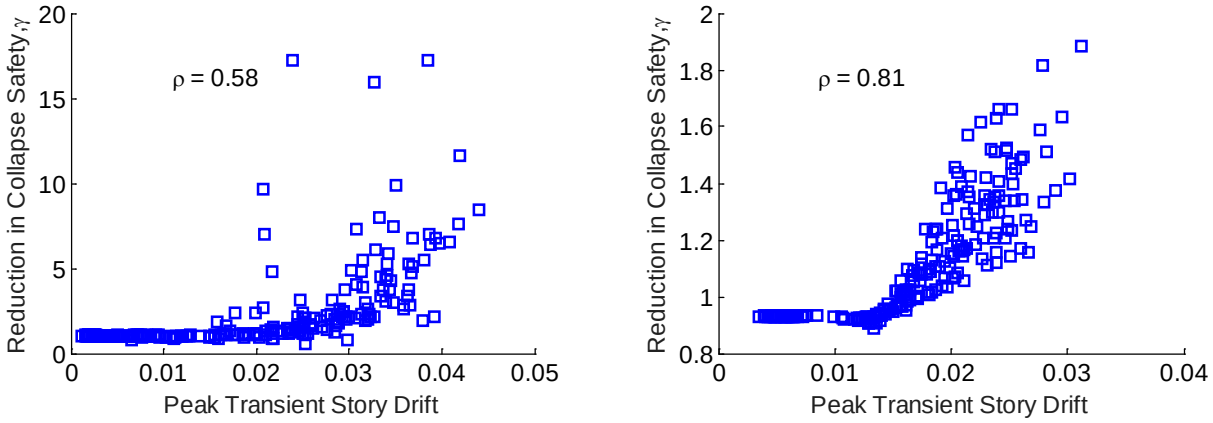

(a) (b)

Fig. 7 – Relationship between the reduction in collapse safety of mainshock-damaged building and peak transient drift for (a) full and (b) partial height infill cases

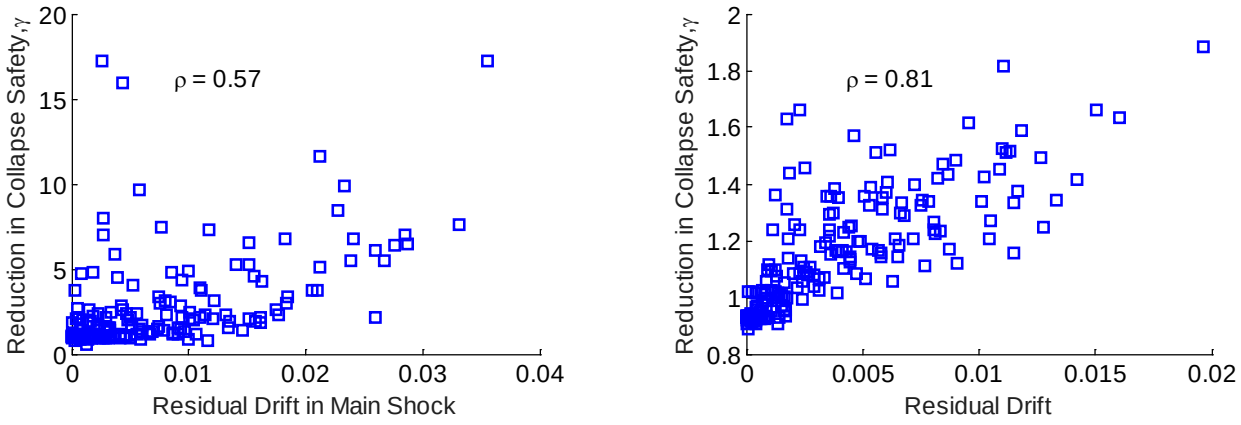

(a) (b)

Fig. 8 – Relationship between the reduction in collapse safety of mainshock-damaged building and residual drift

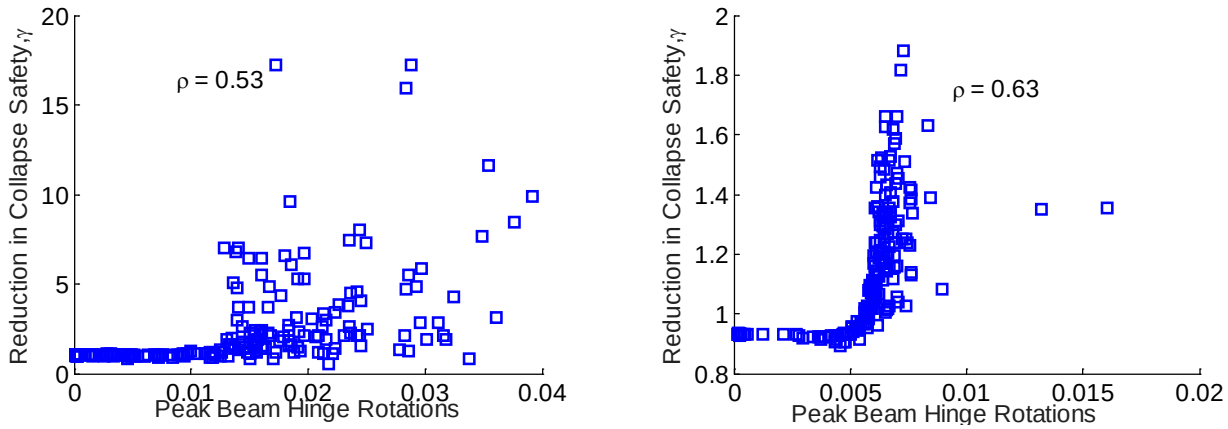

(a) (b)

Fig. 9 – Relationship between the reduction in collapse safety of mainshock-damaged building and maximum beam hinge rotation

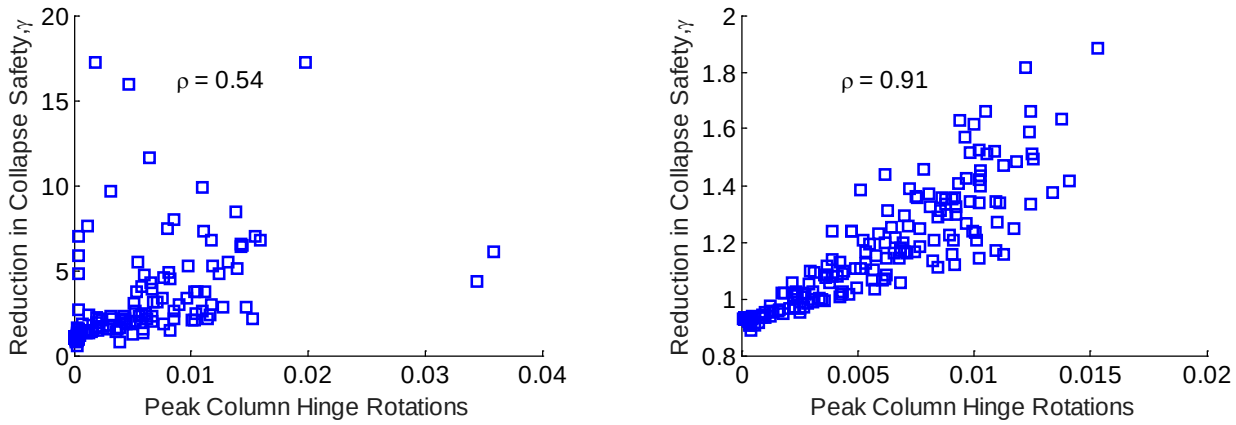

(a) (b)

Fig. 10 – Relationship between the reduction in collapse safety of mainshock-damaged building and maximum column hinge rotation

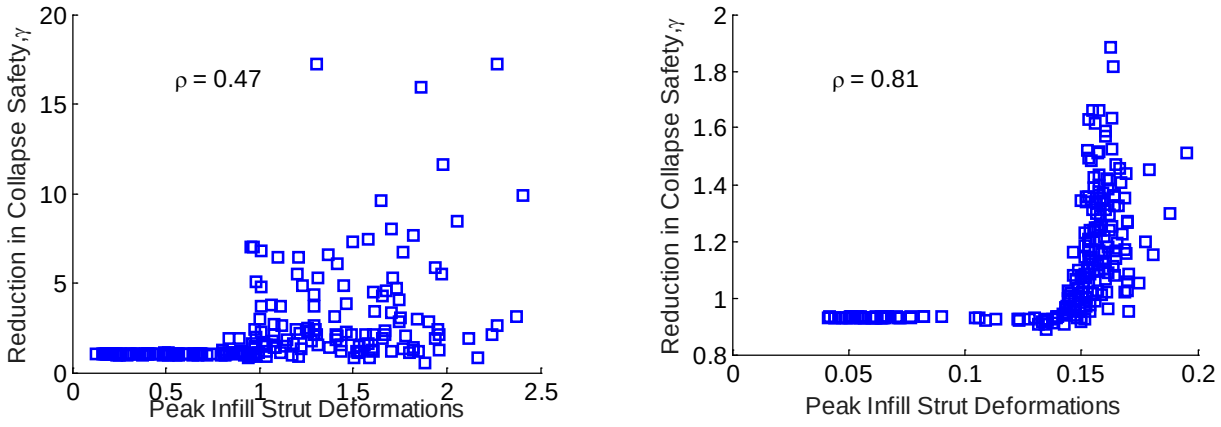

(a) (b)

Fig. 11 – Relationship between the reduction in collapse safety of mainshock-damaged building and maximum infill strut deformation

5. Conclusions

This study quantifies the aftershock collapse safety of two 6-story reinforced concrete frame buildings with infills through the application of mainshock-aftershock *IDAs* to collapse. The building variants differ only in the manner in which the infill panels are configured. One is constructed with full-height infill panels and the second with the infill panels terminating at the second story. The ratio between the median spectral acceleration at collapse for a building in its intact state to that of its damaged state, is used as a measure of reduced collapse safety resulting from mainshock damage. The increase in the conditional probability collapse at the ground motion intensity corresponding to the (mainshock) *MCE* hazard level is also used to quantify the decline in collapse vulnerability due to mainshock damage. After assessing the collapse performance of the intact buildings, a statistical distribution of the aftershock collapse capacity was obtained by subjecting each building to multiple ground motion sequences (one sequence consists of two ground motions) in which the mainshock was held at a single intensity and the aftershock intensity was increased until collapse occurred. Each building was analyzed using 9680 mainshock-aftershock collapse sequences. The mainshock intensity was varied to evaluate the effect of the level and distribution of mainshock damage on the aftershock collapse safety. The resulting dataset was used to describe the residual collapse capacity of the structure as a function of mainshock intensity. The soft and weak story building was found to be more vulnerable to incremental changes in mainshock intensity than the one with full-height infill. This finding is consistent with response demands recorded during the mainshock analyses, which showed that the damage to the building with partial height infill panels tended towards the formation of a single story mechanism. The mainshock (global and local) response demands of the soft story building was found to have a greater correlation with the aftershock collapse safety than the building with full height panels. Of the component response parameters, the peak column hinge rotation was found to have the highest correlation with the aftershock collapse capacity for both building types.

6. References

[1] Wooddell, KE and Abrahamson, NA (2014): Classification of Mainshocks and Aftershocks in the NGA-West2 Database, *Earthquake Spectra*, 30(3), 1257–1267.

[2] Tesfamariam, S, Goda, K and Mondal, G, (2015): Seismic vulnerability of RC frame with unreinforced masonry infill due to mainshock-aftershock earthquake sequences. *Earthquake Spectra*, 31(3) 1427-1449.

[3] Yeo, GL and Cornell, CA (2009): A probabilistic framework for quantification of aftershock ground-motion hazard in California: Methodology and Parametric Study. *Earthquake Engineering and Structural Dynamics*, 38(1), 45-60.

[4] Ebrahimian, H, Jalayer, F, Asprone, D, Lombardi, AM, Marzocchi, W, Prota, A and Manfredi, G (2014): Adaptive daily forecasting of seismic aftershock hazard. *Bulletin of the Seismological Society of America*, 104(1), 145-161.

[5] Luco, N, Bazzurro, P and Cornell, CA (2004): Dynamic versus static computation of the residual capacity of a mainshock-damaged building to withstand an aftershock. Proceedings of the 13th World Conference on Earthquake Engineering, Vancouver, British Columbia.

[6] Ryu, H, Luco, N, Uma, SR. and Liel, AB (2011): Developing fragilities for mainshock-damaged structures through incremental dynamic analysis. Ninth Pacific Conference on Earthquake Engineering Building an Earthquake-Resilient Society, Paper 225.

[7] Ruiz-García, J and Aguilar, J (2014): Aftershock seismic assessment taking into account postmainshock residual drifts. *Earthquake Engineering & Structural Dynamics*, 44(9), 1391-1407.

[8] Raghunandan, M, Liel, A, and Luco, N (2015): Aftershock collapse vulnerability assessment of reinforced concrete frame structures. *Earthquake Engineering & Structural Dynamics* 44(3), 419-439.

[9] Jeon, J, DesRoches, R, Laura, L and Brilakis, I, (2015): Framework of aftershock fragility assessment-case studies: older California reinforced concrete building frames. *Earthquake Engineering Structural Dynamics*, DOI: 10.1002/eqe.2599.

[10] Li, Q. and Ellingwood, B. R (2007): Performance evaluation and damage assessment of steel frame buildings under mainshock-aftershock earthquake sequences. *Earthquake Engineering & Structural Dynamics* 36, 405-427.

[11] Li, Y, Song, R. and van de Lindt, J (2014): Collapse fragility of steel structures subjected to earthquake mainshock-aftershock sequences. *ASCE Journal of Structural Engineering*, 140(12), 04014095-1.

[12] Nazari, N, van de Lindt, J, and Y. Li (2015). Effect of Mainshock-Aftershock Sequences on Woodframe Building Damage Fragilities. *ASCE Journal of Performance of Constructed Facilities*, 29(1), 04014036.

[13] Indian Standard (2000): Criteria for earthquake resistant design of structures. IS 1983 2000, New Delhi, India.

[14] Burton, H (2014): A rocking spine for enhanced seismic performance of concrete frames with infills. Ph.D. Dissertation, Dept. of Civil and Environmental Engineering, Stanford Univ., Stanford, CA.

[15] Sharma, ML, Wason, HR, and Dimri, R (2003): Seismic zonation of the Delhi region for bedrock ground motion. *Pure Applied Geophysics*, 16, 2381-2398.

[16] Ibarra, LF, Medina, RA, and Krawinkler, H (2005): Hysteretic models that incorporate strength and stiffness deterioration. *Earthquake Engineering Structural Dynamics*, 34(12), 1489–1511.

[17] Haselton, CB, Liel, AB, Lange, SL, and Deierlein, G (2008): Beam-column element model calibrated for predicting flexural response leading to global collapse of RC frame buildings. Pacific Earthquake Engineering Research Center; Berkeley, CA.

[18] Saneinejad, A, and Hobbs, B (1995): Inelastic design of infilled frames. *Journal of Structural Engineering*, 121(4), 634–650.

[19] Burton, H, and Deierlein, GG (2014): Simulation of seismic collapse in nonductile reinforced concrete frame buildings with masonry infills. *Journal of Structural Engineering*, 10.1061/(ASCE)ST.1943-541X.0000921.

[20] ASCE (2007): Seismic rehabilitation of existing buildings. ASCE/Structural Engineering Institute (SEI) 41, Reston, VA.

[21] Elwood, K., et al. (2007): Update to ASCE/SEI 41 concrete provisions. *Earthquake Spectra*, 23(3), 493–523.

[22] FEMA (2009): Quantification of building seismic performance factors. FEMA P695, Applied Technology Council, Redwood City, CA.